Cholesterol-Sphingomyelin Interactions: A Molecular Dynamics Simulation Study

Tomasz Róg*† and Marta Pasenkiewicz-Gierula*

*Department of Biophysics, Faculty of Biotechnology, Jagiellonian University, Kraków, Poland; and †Biophysics and Statistical Mechanics Group, Laboratory of Computational Engineering, Helsinki University of Technology, Helsinki, Finland

ABSTRACT Stearoylsphingomyelin (SSM) bilayers containing 0, 22, and 50 mol % cholesterol (Chol) and a pentadecanoyl-stearoylphosphatidylcholine (15SPC) bilayer containing 22 mol % Chol were molecular dynamics simulated at two temperatures (37°C and 60°C). 15SPC is the best PC equivalent of SSM. The Chol effect on the SSM bilayer differs significantly from that on the 15SPC bilayer. At the same temperature and Chol content, H-bonding of Chol with SSM is more extensive than with 15SPC. SSM-Chol H-bonding anchors the OH group of Chol in the lower regions of the SSM-Chol bilayer interface. Such a location strengthens the influence of Chol on the SSM chains. In effect, the phase of the SSM-Chol bilayer containing 22 mol % Chol at 37°C is shifted from the gel to the liquid-ordered phase, and the bilayer displays similar properties below and above the main phase-transition temperature for a pure SSM bilayer of ~45°C. In contrast, due to a higher location, Chol is not able to change the phase of the 15SPC-Chol bilayer, which at 37°C remains in the gel phase. Chol affects both the core and interface of the SSM bilayer. With increasing Chol content, the order of SSM chains and hydration of SSM headgroups increase, whereas polar interactions between lipids decrease.

INTRODUCTION

Sphingomyelins (SM), phosphatidylcholines (PC), and cholesterol (Chol) constitute three major classes of lipids in the outer leaflet of the animal cell membrane. These lipids are nonuniformly distributed in the membrane plane and form domains presumably enriched in SM and Chol (rafts) and areas enriched in PC (1). Rafts were shown to play a role in numerous biological functions, and for this reason, interactions between SM and Chol that may lead to raft formation and stabilization are of great interest to membrane biophysicists. An excellent overview of the current biophysical viewpoint on rafts is given in Pandit et al. (2,3, and references cited therein).

The chemical structures of PC and SM molecules are shown in Fig. 1. Both phospholipids have the phosphorylcholine group as the polar head but they differ in the backbone and acyl chain regions. As recently summarized by Ramstedt and Slotte (4), the main ''functional'' difference between the backbone regions comes from two hydrogen (H)-bond donor groups, amide and hydroxyl, which, in addition to the H-bond-accepting carbonyl group, are present in SM; in contrast, PC has only H-bond-accepting carbonyl groups in this region. Acyl chains of SM and PC differ in the length and presence of *cis* double bonds. In SM and PC, the chains are commonly 16–24 and 16–18 carbon atoms long, respectively. If the C4=C5 bond on SM (cf. Fig. 1 *b*) is not considered, the occurrence of *cis* double bonds in PC chains is 5–10 times higher than in SM chains. If a *cis* double bond occurs in the acyl chain of SM, it is usually located further away from the headgroup than in the case of PC (4) and its effect on the properties of a SM bilayer is small (5).

The formation of rafts may result from a preference of Chol to interact with SM over PC. This preference can be attributed to the structural differences between SM and PC outlined above. Chol-phospholipid H-bonding that in PC-Chol bilayers goes only via the hydrogen atom of the Chol hydroxyl group (OH-Chol) (6–8) is expected to be more effective in SM-Chol bilayers. Indeed, experimental studies demonstrated formation of H-bonds between Chol and SM (9) that involves, in addition to OH-Chol, the SM amide group as H-bond donor (10). Molecular dynamics (MD) simulation studies (11–13) are in line with experimental indications (14) that in SM aggregates, the hydroxyl group of SM is involved mainly in intramolecular, and the amide group in intermolecular, H-bonding. Nonetheless, Holopainen et al. (15) did not detect any specific interactions between SM and Chol using fluorescence spectroscopy.

In PC bilayers, Chol is known to induce higher ordering of PC chains (ordering effect) and higher surface density of the bilayer (condensing effect). Both effects are stronger in saturated than in unsaturated bilayers (16–20). In desorption experiments, Ramstedt and Slotte (21) demonstrated that the strength of PC-Chol interactions decreases with increasing length of PC chains to >14 carbon atoms but that of SM-Chol does not depend on the SM chain length. Comparative studies of the Chol effect on bilayers composed of SM and PC of matching chains revealed a slower rate of Chol desorptions from SM bilayers (21) as well as higher order (22) and condensation (23) in SM bilayers.

Computer simulation studies of the effect of Chol on lipid bilayers have been carried out mainly on PC-Chol bilayers (8,17,18,20,24–31), but recently, SM (11–13,33)

Submitted January 9, 2006, and accepted for publication August 3, 2006.

Address reprint requests to Marta Pasenkiewicz-Gierula, E-mail: mpg@mol.uj.edu.pl.

0006-3495/06/11/3756/12 $2.00

doi: 10.1529/biophysj.106.080887

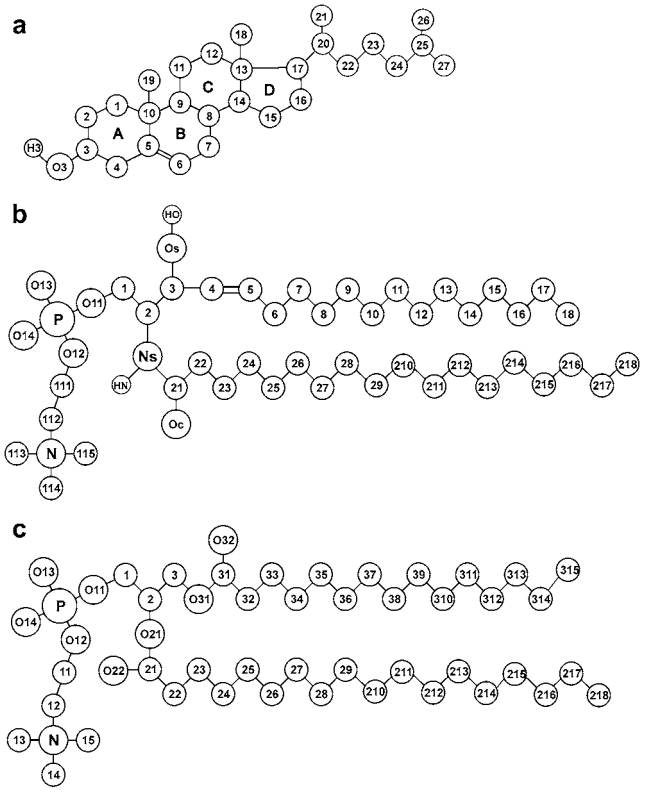

FIGURE 1 Molecular structures with numbered atoms of Chol (*a*), SSM (*b*), and 15SPC (*c*) molecules (the chemical symbol for carbon atoms, C, is omitted). The Chol rings are labeled *A–D*.

and SM-Chol (2,3,34) bilayers have received attention. MD simulations of pure SM bilayers showed extensive intra- and interlipid H-bonding, higher ordering of SM hydrocarbon chains, reduced hydration of SM headgroups, and slower dynamics of SM molecules, compared to PC. SM-Chol bilayers display similar properties at temperatures both below and above the main phase-transition temperature (T_m) for a pure SM bilayer. The OH-Chol group forms H-bonds predominantly with carbonyl (SM-OC), amide (SM-NH), and hydroxyl (SM-OH) groups of SM and, to a lesser degree, with phosphate and glycerol groups. The study of Pandit et al. (3) provides an unexpected result suggesting that Chol locates between SM-rich and dioleoylphosphatidylcholine (DOPC)-rich domains in the DOPC-SM-Chol bilayer with a 1:1:1 composition, and accelerates the process of domain formation; the smooth α-face of Chol is oriented toward SM molecules.

In this article, we employ a MD simulation methodology to study the effect of Chol on the stearoylsphingomyelin (SSM) bilayer at two temperatures (37°C and at 60°C) and two Chol concentrations (22 and 50 mol % Chol), and to compare the properties of the SSM-Chol bilayer with those of the pentadecanoylstearoylphosphatidylcholine (15SPC)-bilayer-containing Chol (PC-Chol bilayer), at 37°C. SSM and 15SPC have saturated hydrocarbon chains of matching lengths and similar main phase-transition temperatures (~45°C). The questions we address in this study concern 1), the effect of Chol on the SSM bilayer at temperatures above T_m (60°C), i.e., in the liquid-crystalline phase, by comparing the pure SSM bilayer with the SSM bilayer containing 22 mol % Chol; 2), the effect of Chol concentration (22 and 50 mol %) on the SSM bilayer at the physiological temperature of 37°C; and 3), the effect of 22 mol % Chol on the SSM bilayer at 37°C and 60°C. A separate issue, perhaps the least explored so far, is 4), a comparison between the effect of Chol on 15SPC and that on SSM bilayers at the same Chol concentration of 22 mol % and the physiological temperature. This comparison indicates that even though main phase-transition temperatures of 15SPC and SSM bilayers are similar, Chol differently affects the phase state of both bilayers, most likely due to its different localization in the bilayers.

METHOD

Simulation system

Four bilayers were constructed. They consisted of 1), 72 SSM (N-stearoyl-*d-erythro*-sphingosylphosphorylcholine) and 72 Chol molecules (SM-Chol50); 2), 72 SSM and 20 Chol molecules (SM-Chol20); 3), 72 pentadecanoyl-stearoylphosphatidylcholine (15:0-18:0-PC, 15SPC) and 20 Chol molecules (PC-Chol); and 4), 72 SSM molecules (SM). 15SPC is the best PC equivalent of SSM because it has hydrocarbon chains of matching lengths and a similar main phase-transition temperature. For this reason, the PC-Chol bilayer, built of 15SPC and Chol molecules, was selected as a reference system. Three of the bilayers (SM-Chol50, SM-Chol20, and PC-Chol) were MD simulated at 37°C and two of the bilayers (SM and SM-Chol20) were MD simulated at 60°C. Thus, the SM-Chol20 bilayer was simulated at two temperatures (details are given below).

The initial structure of the SSM molecule was built from the crystal structure of β-D-galactosyl-N-octadecanoyl-D-sphingosine (35) using InsightII software (Accelrys, San Diego, CA) by replacing the sugar group with phosphorylcholine. This procedure ensured the *d-erythro-* (2S, 3R) configuration of the sphingosine moiety as well as the *trans* conformation of the double bond between C4 and C5 (cf. Fig. 1). The initial structures of SSM and SSM-Chol bilayers were constructed in three steps. 1), SSM or SSM and Chol molecules were placed on the *x,y* plane to form a regular layer (the *x,y* plane) in such a way as to avoid van der Waals contacts. In the bilayers containing Chol, the Chol molecules were uniformly distributed and separated from one another by SSM molecules. 2), The second layer was obtained from the first by 180° rotation and shifting to reduce the free volume. 3), The bilayer was hydrated with 1955 water molecules, i.e., ~27/SM, by adding two layers of water stretching from the average positions of the carbonyl oxygen atoms outward. The PC-Chol bilayer was constructed following the same procedure. Each bilayer was simulated for 20 ns using AMBER 5.0 (36). Except in the case of the PC-Chol bilayer (cf. the Equilibration section), the final 15-ns fragments of the generated trajectories were used for analyses. The structure and numbering of atoms in Chol, SSM, and 15SPC molecules are shown in Fig. 1.

Simulation parameters

For lipid molecules, optimized potentials for liquid simulations (OPLS) parameters (37) were used. Pasenkiewicz-Gierula et al. described the procedure for supplementing the original OPLS base with the missing parameters for atom types in the PC headgroup (38) and Chol (8); the numerical values for the atomic charges of PC and Chol are also given. The numerical values for the atomic charges and other parameters of SSM groups not present in the PC

molecule were approximately the same as for corresponding groups of peptides in the OPLS. The atomic charges on the SSM were slightly readjusted to give the net charge zero (the numerical values for the charges are given in Supplementary Material). The united-atom approximation was applied to the CH, CH_2, and CH_3 groups of SSM, PC, and Chol. The hydroxyl and amide groups of Chol, water, and SSM were treated with full atomic details. For water, TIP3P parameters were used (39).

Simulation conditions

The SHAKE algorithm (40) was used to preserve the bond lengths of the OH and NH groups of water, Chol, and SSM molecules, and the time step was set at 2 fs (41). The nonbonded interactions were evaluated under three-dimensional periodic boundary conditions using the particle-mesh Ewald (PME) summation (42). A real cutoff of 12 Å with the usual minimum image convention, β spline interpolation order of 5, and direct sum tolerance of 10^{-6} were used. The list of nonbonded pairs was updated every 25 steps.

The MD simulations were performed in the NPT ensemble, at a pressure of 1 atm and two temperatures (37°C and 60°C). For the first group of bilayers, i.e., SM-Chol50, SM-Chol20, and PC-Chol bilayers, the system temperature was 37°C (310 K), which is below T_ms for both pure SSM and 15SPC bilayers of ~45°C (43) and ~43°C (44), respectively. These simulations enabled us to compare bilayers composed of PC and SM of matching chains and containing the same amount of Chol at the physiological temperature and also to assess the effect of the increased Chol concentration on the SSM-Chol bilayer. For the second group of bilayers, i.e., SM and SM-Chol20 bilayers, the system temperature was 60 C (333 K) (the SM-Chol20 bilayer simulated at 60 C is referred to as SM-Chol20*). These simulations enabled us to determine the effect of Chol on the SSM bilayer in the liquid-crystalline state. The temperatures of the solute and solvent were controlled independently. Both the temperatures and pressure of the systems were controlled by the Berendsen method (45). The relaxation times for temperatures and pressure were set at 0.4 and 0.6 ps, respectively. The pressure was controlled anisotropically as implemented in the AMBER 5.0 package (36). In this implementation, both the shape and the volume of the simulation box are changed by rescaling the box size and the coordinates of the atoms in each direction independently, keeping one-third of the trace of the stress tensor at the target value.

RESULTS

Characterization of the membrane

Equilibration

In this study, analyses of the bilayer systems concern either short-range interactions at the bilayer interface (mainly H-bonding) or hydrocarbon chain order and tilt in the bilayer core. These quantities depend on the average cross-sectional area available to a lipid molecule in the bilayer. Thus, for the purpose of this study, the convergence of the surface area/lipid is an adequate indicator of the bilayer equilibration (supporting data can be found in Supplementary Material). Fig. 2 shows time profiles of the SM-Chol50 bilayer potential energy (Fig. 2 *a*), and the surface area (Fig. 2 *b*) as well as the time profile of the surface area of the PC-Chol bilayer (Fig. 2 *c*), from the onset of simulation until 20 ns. At a steady state, these parameters should remain constant. As Fig. 2, *a* and *b*, shows, for the SM-Chol50 bilayer both the potential energy and the area of the simulation box stabilized within the first ~4.0 ns of MD simulation, so we concluded that the SM-Chol50 bilayer had reached a steady state at 4 ns.

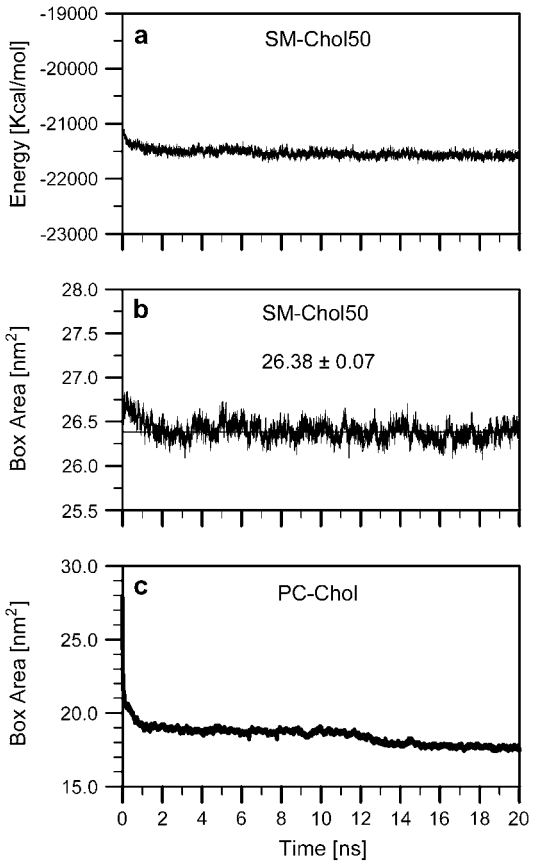

FIGURE 2 Time profiles of the SM-Chol50 bilayer potential energy (*a*), and the simulation box surface area of the SM-Chol50 bilayer (*b*) and the PC-Chol bilayer (*c*), from the onset of MD simulations. The thin line in panel *b* indicates the average value after equilibration of the SM-Chol50 simulation box surface area of 26.4 ± 0.1 nm^2.

Similar time profiles were obtained for the remaining SSM-Chol and SSM bilayers (data not shown). These bilayers equilibrated within similar time periods. For analyses of the SSM and SSM-Chol bilayers, the last 15-ns trajectory fragments generated between 5 and 20 ns of MD simulation were used. Reported average values are averages over the simulation time and the ensemble of molecules or their fragments. Errors in the derived average values are standard error estimates obtained from the block averaging procedure.

The approach to the thermally equilibrated state of the PC-Chol bilayer was much slower than that of the SSM-Chol bilayers. A large initial area of the simulation box (Fig. 2 *c*) allowed the bilayer to relax to the preferred configuration at the steady state. However, the area kept decreasing for at least 15 ns of the simulation and it might not have reached a steady value even during 20 ns of simulation. Nevertheless, we used the last 5-ns fragment of the trajectory for analyses, because the decrease in the area was then not that apparent (Fig. 2 *c*). Results of these analyses were used for limited comparisons with the SSM-Chol bilayers to show contrasts. Snapshots of SM-Chol20 and PC-Chol bilayers at the end of the respective trajectories are shown in Fig. 3. There is a

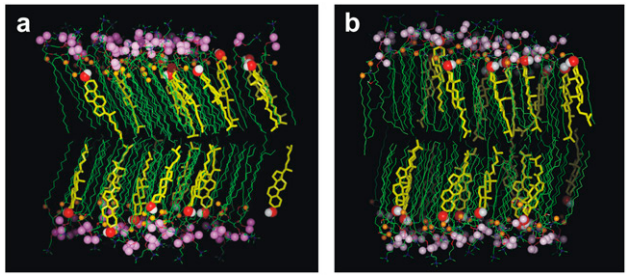

FIGURE 3 Snapshots of PC-Chol (*a*) and SM-Chol20 (*b*) bilayers at the end of their 20-ns MD trajectories. Cholesterol molecules are shown as yellow sticks with the OH group in the standard colors of a CPK model. The nonester phosphate oxygen atoms, O14 and O13 (Fig. 1), are larger pink spheres, and the carbonyl oxygen atoms O22 and O32 (Fig. 1) are smaller brown spheres.

striking difference between tilting of chains in both bilayers. In the PC-Chol bilayer, the collective tilt (for details, see below) of the 15SPC chains and Chol is ~17°, which means that the bilayer is in the gel phase (46). The 15SPC chains, as well as Chol, are tilted in opposite directions in both bilayer leaflets, which can be attributed to an unequal length of the 15SPC chains and possibly the way the initial structure was constructed. A similar pleated structure was obtained in a MD simulation of a gel-phase dipalmitoylphosphatidylcholine bilayer (47). In the SM-Chol20 bilayer, the SSM chains are highly ordered but their collective tilt, as well as that of Chol, is zero; this indicates that the SM-Chol20 bilayer is in the liquid-ordered phase. Even though the equilibration of the PC-Chol bilayer is not certain, numerical results characterizing the global properties of the bilayer as well as the bilayer core are given in Table 1. The values of parameters describing interactions involving polar groups of 15SPC and Chol, as well as water in the bilayer interface, are given in Tables 2–4. We believe that the values of these parameters obtained for the last 5 ns of MD simulation are not far from the steady-state values due to a substantial motional freedom of the polar groups and water molecules in the bilayer interface.

Thickness

The thickness of a bilayer was evaluated as the distance between average positions of phosphorus (P) atoms in the two leaflets of the bilayer (P-P distance). Average values for the bilayers studied here are given in Table 1 and compared with those for the dimyristoylphosphatidylcholine (DMPC) bilayer containing 22 mol % Chol (DMPC-Chol bilayer) (30). As expected, when compared at the same temperature, the SSM bilayer containing Chol is thicker than the pure one. A result worth noting is that the thickness of all SSM bilayers containing Chol is practically the same, irrespective of the Chol concentration and the bilayer temperature. The values for the P-P distance in the SM and SM-Chol50 bilayers of 43.5 and 46.5 Å, respectively, agree perfectly with those obtained by x-ray diffraction (48).

Surface density

The surface density of the membrane was calculated by dividing the total mass of all membrane lipids by the surface area of the simulation box. Average values for the bilayers are given in Table 1 and compared with those for the DMPC-Chol bilayer (31). Again, as expected, when compared at the same temperature, the surface density of the SSM bilayer containing Chol is larger than the pure one. The surface

TABLE 1 Average membrane parameters

	SM-Chol50	SM-Chol20	SM-Chol20*	SM	PC-Chol	DMPC-Chol
Temperature (K)	310	310	333	333	310	310
S_{mol}						
SPH (γ-chain)	0.78 ± 0.01	0.67 ± 0.01	0.68 ± 0.01	0.51 ± 0.01	0.48 ± 0.01	0.40 ± 0.01
S (β-chain)	0.81 ± 0.01	0.68 ± 0.01	0.69 ± 0.01	0.49 ± 0.01	0.43 ± 0.01	0.45 ± 0.01
No. *gauche* rotamers						
SPH (γ-chain)	1.01 ± 0.05	0.96 ± 0.05	0.82 ± 0.05	1.52 ± 0.05	2.18 ± 0.05	2.2 ± 0.1
S (β-chain)	2.42 ± 0.05	2.19 ± 0.05	2.05 ± 0.05	2.64 ± 0.05	1.25 ± 0.05	2.3 ± 0.1
Tilt angle (°)						
SPH (γ-chain)	8.0 ± 0.5	14.0 ± 0.5	14.5 ± 0.5	20.0 ± 0.5	14.0 ± 0.5	22.0 ± 0.5
S (β-chain)	8.5 ± 0.5	14.5 ± 0.5	15.2 ± 0.5	21.0 ± 0.5	15.0 ± 0.5	20.0 ± 0.5
Collective tilt (°)	~0 ± 4	~0 ± 4	~0 ± 4	~0 ± 4	~17 ± 1	~0 ± 5
Area (Å^2)	73.2 ± 0.5	52.5 ± 0.5	51.8 ± 0.5	48.0 ± 0.5	49.2 ± 0.5	64 ± 1
Surface density ($\times 10^{-7}$ g/cm^2)	2.53 ± 0.01	2.57 ± 0.01	2.64 ± 0.01	2.27 ± 0.01	2.93 ± 0.01	2.04 ± 0.01
P-P distance (Å)	46.5 ± 0.5	46.7 ± 0.5	46.6 ± 0.5	43.5 ± 0.5	48.5 ± 0.5	35.1 ± 0.1

Average values of the molecular order parameter, S_{mol}; number of *gauche*/chain (No. *gauche*); chain tilt angle (Tilt angle); collective tilt angle (Collective tilt); surface area available to the lipid headgroup (Area); membrane surface density; and distance between average positions of phosphorus (P) atoms in the two leaflets of a bilayer (P-P distance), for the sphingosine- (SPH) and stearoyl- (S) chain of SSM in SM-Chol50, SM-Chol20, SM-Chol20*, and SM bilayers. For comparison, results for the DMPC-Chol bilayer (30,31) are also given. The same parameters were obtained for the PC-Chol bilayer (β- and γ-chains of 15SPC), which might not have reached a steady state during the simulation time (cf. Results and Fig. 2). The tilt angle was calculated according to the definition in Róg and Pasenkiewicz-Gierula (20). The collective tilt angle is an average angle between a phospholipid chain and the bilayer normal, averaged over all chains in the bilayer. The errors in the average values are standard error estimates.

TABLE 2 Interactions in the membrane/water interface

	SM-Chol50 310 K	SM-Chol20 310 K	SM-Chol20* 333 K	SM 333 K	PC-Chol 310 K
Interlipid					
H-bonds					
SM-SM	0.22	0.56	0.59	0.66	–
SM-Chol (PC-Chol)	0.64/Chol	0.91/Chol	0.78/Chol	–	0.28/Chol
Charge pairs					
SM-SM (PC-PC)	1.29	1.74	1.79	1.85	1.58
SM-Chol (PC-Chol)	0.61/Chol	0.58/Chol	0.47/Chol	–	1.02/Chol
Water bridges					
SM-SM (PC-PC)	0.71	1.00	0.92	0.86	0.82
SM-Chol (PC-Chol)	0.19/Chol	0.13/Chol	0.13/Chol	–	0.14/Chol
Chol-Chol	0.04/Chol	0.01/Chol	0.01/Chol	–	0.01/Chol
Total					
SM-SM (PC-PC)	2.22	3.30	3.30	3.37	2.40
SM-Chol (PC-Chol)	1.44	1.62	1.38	–	1.44
Intralipid					
H-bonds					
SM-SM	0.47	0.50	0.48	0.50	–
Charge pairs					
SM-SM (PC-PC)	0.19	0.13	0.15	0.14	0.18
Water bridges					
SM-SM (PC-PC)	0.16	0.14	0.11	0.14	0.16
Total					
SM-SM (PC-PC)	0.82	0.77	0.74	0.78	0.34

The data represent the numbers of SM-SM, PC-PC, SM-Chol, PC-Chol, and Chol-Chol inter- and intralipid H-bonds, water bridges, and charge pairs, as well as the total number of all interactions (Total) per phospholipid or Chol, in SM-Chol50, SM-Chol20, SM-Chol20*, SM, and PC-Chol bilayers. The standard error estimates of the average values do not exceed ± 0.02.

density of SSM-Chol bilayers slightly depends both on the Chol concentration and the bilayer temperature.

Area

In PC bilayers, organization of the membrane/water interface is correlated with the average surface area available to the PC headgroup. This issue is thoroughly discussed in Murzyn et al. (49). To check whether similar correlations can be found in bilayers consisting of other lipids, average surface areas available to SSM and 15SPC headgroups were calculated by dividing the surface area of each bilayer by the number of SSM or 15SPC molecules in one bilayer leaflet (Table 1). The correlation between the available area and the organization of the interfacial region is discussed below.

Bilayer core

Chain order

Values of the molecular order parameter, S_{mol}, along a hydrocarbon chain are determined both by the *trans-gauche* isomerization (represented by the number of *gauche* rotamers in the chain) and by the ''rigid-body'' chain rotation about the in-plane axis (represented by the chain tilt), averaged over all chains in the bilayer. In the first approximation, the effect of rotational isomerism is cumulative—''disorder'' increases along the chain, whereas the effect of the rigid-body rotation is constant along the chain. In the liquid-crystalline phase (ordered or disordered), the average angle of chains with respect to the bilayer normal (collective tilt, Table 1) is zero, indicating that the mean orientations of the chains relative to the normal are almost randomly distributed within a cone. The cone angle corresponds to the largest tilt angle. Due to internal flexibility of hydrocarbon chains, an average angular amplitude of the chain rotation (average tilt) inside the cone cannot be measured experimentally, so individual contributions of both rotations to S_{mol} cannot be separated. In MD simulations, however, they can be treated individually, and the Chol effect on each of the three quantities can be estimated. Our previous studies on PC-Chol bilayers (30,32,50) indicate a strong positive correlation between tilts of sterol molecules and their neighboring saturated acyl chains. However, the effect of Chol on the *trans-gauche* isomerization is less straightforward (30,32).

In this study, S_{mol} and chain tilt, which is a measure of chain orientational fluctuations, were calculated as in our previous articles (20). Average values of S_{mol}, tilt, and numbers of *gauche* rotamers per chain for all bilayers studied here, together with those for the DMPC-Chol (30) bilayer, are given in Table 1. Profiles of S_{mol} along the sphingosine- (SPH) and stearoyl- (S) chains of SSM in the four SSM bilayers are shown in Fig. 4. Similarly, as in the saturated DMPC bilayer (30), Chol increases the order and decreases the tilt of SSM chains. The magnitude of both effects practically does not depend on the bilayer temperature but on

TABLE 3 Lipid-water interactions

	SM-Chol50	SM-Chol20	SM-Chol20*	SM	PC-Chol
H-bonds					
Op	3.98	3.85	3.78	3.58	3.86
SM-OC (Oc)	0.91	0.67	0.71	0.51	0.62
SM-OH	0.55	0.34	0.32	0.28	–
	(0.35/0.24)	(0.23/0.11)	(0.19/0.13)	(0.17/0.11)	
SM-NH	0.36	0.30	0.26	0.19	–
Total/Chol	2.13	2.10	2.12	–	2.15
Total/lipid	5.80	5.16	5.07	4.56	4.48
H-bonded water	5.51	4.65	4.61	4.13	4.07
Choline water	6.88	6.56	6.73	6.34	6.63
Bound water	12.39	11.21	11.34	10.47	10.70

The data represent the numbers of H-bonds between water and polar groups of SM and PC per group and per SM and PC (Total/lipid), and between water and Chol per Chol (Total/Chol); total numbers of H-bonded water molecules (H-bonded water), water molecules in a clathrate around the choline groups (Choline water), and water molecules bound to SM and PC (H-bonded and clathrating) (Bound water) per SM and PC in SM-Chol50, SM-Chol20, SM-Chol20*, SM, and PC-Chol bilayers. Numbers in parentheses indicate cases in which the SM-OH group is the H-bond donor/acceptor. See Table 4 note for definitions of Op and Oc. The standard error estimates of the average values do not exceed ±0.02 in the case of H-bonds and ±0.03 in the case of the Choline water.

the Chol content. Probability profiles of the *gauche* conformation along the SPH- and S-chain in SM and SM-Chol20* bilayers are shown in Fig. 5. In contrast to another saturated (DMPC) bilayer (30), Chol decreases the average number of *gauche* conformations in both chains of SSM (Table 1) as well as the *gauche* probability for all torsion angles except the last two (15 and 16) in the S-chain, for which the probability is increased (Fig. 5). (These torsion angles are located in the bilayer below the Chol ring system.) Thus, Chol induces higher order of SSM chains by decreasing their tilt and probability of *gauche* conformation.

Membrane/water interface

The membrane interfacial region is composed of lipid polar groups and water molecules. Phosphate, carbonyl, hydroxyl, and amide groups of phospholipids and Chol make H-bonds

TABLE 4 Chol-Phospholipid hydrogen bonds

	SM-Chol50	SM-Chol20	SM-Chol20*	PC-Chol
Op	0.21	0.22	0.14	0.17
SM-OC (Oc)	0.16	0.21	0.12	0.11
SM-OH	0.10	0.21	0.18	–
SM-NH	0.17	0.27	0.34	–
Total	0.64	0.91	0.78	0.28

The data are numbers of H-bonds between Chol and polar groups of SM and PC per Chol and their sum (Total) in SM-Chol50, SM-Chol20, SM-Chol20*, and PC-Chol bilayers. Op stands for both nonester phosphate oxygen atoms of SM and PC (O14 and O13 (Fig. 1, *b* and *c*)), and Oc stands for both carbonyl oxygen atoms of PC (O22 and O32 (Fig. 1 *c*)). The standard error estimates of the average values do not exceed ±0.02.

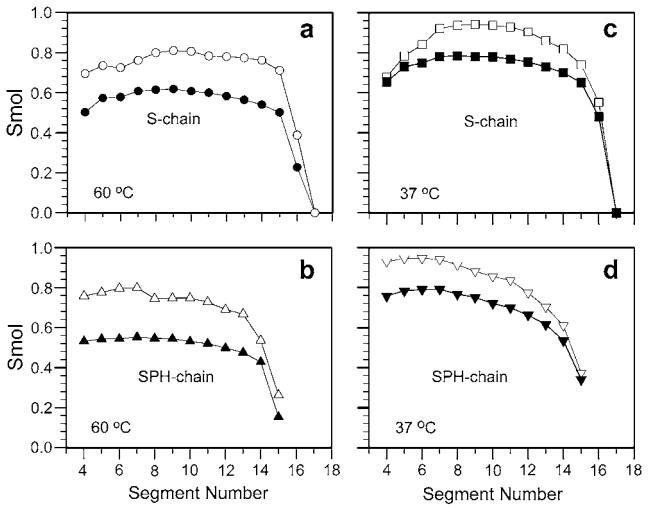

FIGURE 4 Molecular order parameter (S_{mol}) profiles calculated for the S-chain (stearoyl) (*a* and *c*) and SPH-chain (sphingosine) (*b* and *d*) in SM (●, ▲) and SM-Chol20* (○, △) bilayers (*a* and *b*), and in SM-Chol50 (□,▽) and SM-Chol20 (■, ▼) bilayers (*c* and *d*).

with water. The choline group attracts and rearranges water molecules so they form clathrates around it. The lipid polar groups also interact with one another by forming direct H-bonds and charge pairs. Furthermore, they interact via water molecules (water bridges) that are simultaneously H-bonded to two groups of the same (intramolecular) or different (intermolecular) lipids. In this study, we use the same geometrical definitions of H-bonding, water bridging, and charge pairing as in our previous articles (38,49,51).

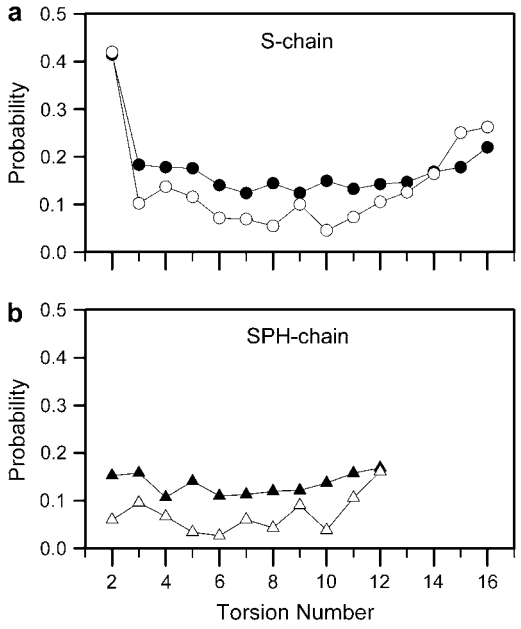

FIGURE 5 Probabilities of *gauche* conformations along the S-chain (*a*) and SPH-chain (*b*) in SM (●, ▲) and SM-Chol20* (○, △) bilayers.

Lipid-water interactions

The number of SSM-water H-bonds (Table 3) is strictly correlated with the area available to the SSM headgroup (Table 1) and increases with increasing Chol content. The number ranges from 4.56/SSM in the SM bilayer to 5.84/SSM in the SM-Chol50 bilayer and is higher than that in the PC-Chol bilayer, of 4.48/PC (Table 3). As expected, water makes H-bonds predominantly with the nonester phosphate oxygen (Op, i.e., O14 and O13, cf. Fig.1, *b* and *c*) atoms (~2/Op) of both SSM and 15SPC, and unexpectedly many with SM-OC in the SM-Chol50 bilayer of 0.91/SM-OC (Table 3). The number of water molecules H-bonded to the phospholipid ranges from 4.13/SSM in the SM bilayer to 5.51/SSM in the SM-Chol50 bilayer and is smaller than the number of phospholipid-water H-bonds (Table 3). This indicates formation of inter- and intralipid water bridges. Chol makes similar number of H-bonds with water (~2.12/Chol) in all bilayers; in 73% of them, Chol is an H-bond donor and in 27% an H-bond acceptor. The number of water molecules in clathrates around choline groups in the SM bilayer is smaller than in bilayers containing Chol (Table 3). Thus, as in our previously studied systems (48), there is a weak correlation between the number of water molecules in the clathrate and the surface area (Table 3).

SM-SM and PC-PC interactions

H-bonding

SSM molecules have both H-bond donor (SM-OH and SM-NH) and acceptor (Ops, SM-OC, and SM-OH) groups and can make H-bonds with each other (intermolecular) as well as within one molecule (intramolecular), whereas PC molecules cannot, as they have only H-bond acceptor groups (phosphate, carbonyl). The number of SSM intramolecular H-bonds is similar in all SSM bilayers (~0.5/SSM), either pure or containing Chol (Table 2). The bonds are exclusively made between SM-OH and SM-OC (Table 5). The number of SSM-SSM intermolecular H-bonds is in the range 0.22–0.66/SSM (Table 2). Chol reduces strongly intermolecular H-bonding by increasing the average SSM-SSM distance. Preferences of donor and acceptor groups in H-bonding in pure and Chol-containing SSM bilayers are displayed in Table 5. In brief, in SM-Chol20 and SM-Chol20* bilayers, the SM-OC makes H-bonds both with SM-OH and SM-NH, whereas the SM-OH makes H-bonds predominantly with SM-NH. In the SM bilayer, the SM-OH rarely participates in intermolecular H-bonding. SM-NH is never an acceptor in intermolecular H-bonds.

Charge pairing

A positively charged choline moiety ($N\text{-}CH_3$) can make charge pairs with negatively charged oxygen atoms of both SM and PC. We distinguish between intermolecular and intramolecular charge pairs. In SSM bilayers, intramolecular charge pairs are less frequent than intramolecular H-bonds, whereas intermolecular charge pairs are more frequent than intermolecular H-bonds (Table 2); the latter range from 1.29 to 1.85/SSM or 15SPC. As in the case of H-bonds, the number of intramolecular charge pairs is similar in all bilayers (~0.15/SSM or 15SPC), whereas the number of intermolecular charge pairs decreases with increasing Chol content (Table 2).

Water bridges

Numbers of intra- and intermolecular water bridges in the bilayers are given in (Table 2). These numbers do not differ significantly; they are ~0.86/SSM or 15SPC for intermolecular water bridges and ~0.14/SSM or 15SPC for intramolecular water bridges (Table 2).

TABLE 5 SSM-SSM hydrogen bonds

	SM-Chol50 310 K		SM-Chol20 310 K		SM-Chol20* 333 K		SM 333 K	
	SM-OH	SM-NH	SM-OH	SM-NH	SM-OH	SM-NH	SM-OH	SM-NH
Interlipid								
Op	0.11	0.04	0.10	0.04	0.13	0.06	0.14	0.09
SM-OC	0.03	0.00	0.13	0.12	0.11	0.11	0.06	0.22
SM-OH	0.01	0.03	0.02	0.15	0.02	0.14	0.03	0.13
SM-NH	0.00	0.00	0.00	0.00	0.00	0.00	0.00	0.00
SUM	0.15	0.07	0.25	0.31	0.27	0.32	0.23	0.43
Total	0.22		0.56		0.59		0.66	
Intralipid								
SM-OC	0.47	0.00	0.50	0.00	0.48	0.00	0.50	0.00
OS	0.00	0.00	0.00	0.00	0.00	0.00	0.00	0.00

The data are the numbers of H-bonds between SM groups involved in inter- and intralipid SM-SM H-bonding per group (SUM) and per SM (Total) in SM-Chol50, SM-Chol20, SM-Chol20*, and SM bilayers. Column headings are H-bond donor groups, and items in the lefthand column are H-bond acceptor groups. Op stands for both nonester phosphate oxygen atoms of SM (O14 and O13 (Fig. 1 *b*)), and OS stands for both ester phosphate oxygen atoms of SM (O11 and O12 (Fig. 1 *b*)). SM-OC, SM-NH, and SM-OH are carbonyl, amide, and hydroxyl groups, respectively, of SM. The standard error estimates of the average values do not exceed ±0.02.

SM-Chol and PC-Chol interactions

The OH-Chol group can be both H-bond donor and acceptor; thus, it can make direct H-bonds with both SM and PC. It can also interact with the phospholipids via water bridges and charge pairs. In SSM bilayers containing Chol, the number of direct SSM-Chol H-bonds ranges from 0.64 to 0.91/Chol (Table 2); Chol is an H-bond donor in ~60% of them, and an H-bond acceptor in ~40%. Examples of SSM-Chol H-bonds in the SM-Chol20 bilayer are shown in Fig. 6. Chol makes significantly fewer H-bonds with 15SPC than with SSM; on average, in the PC-Chol bilayer there are 0.28 such bonds per Chol (Table 2). Preferences of OH-Chol to H-bond with certain groups of phospholipids are displayed in Table 4. Numbers of SSM-Chol charge pairs are similar in all SSM-Chol bilayers, they range from 0.47 to 0.61/Chol. In the PC-Chol bilayer, the number is 1.02/Chol. There are fewer SSM-Chol and PC-Chol water bridges than other polar interlipid interactions (Table 2).

Chol-Chol interactions

Both in 15SPC and SSM bilayers containing Chol, Chol-Chol interactions are rare and only via water bridges (Table 2).

Location of OH-Chol

As shown in our previous articles (20,32), the effect of sterol on the PC bilayer is correlated with the average location of the sterol's hydroxyl group in the bilayer interface relative to the average position of the phosphate group. The average vertical position of OH-Chol in the SM-Chol20 bilayer is 0.4 Å below that in the DMPC-Chol bilayer (32) and only 0.1 Å below that in the SM-Chol50 bilayer, which is within the estimated error. However, Chol cannot insert too deeply due to the formation of H-bonds between OH-Chol and polar groups in the SSM backbone, which anchor Chol at a certain position. In the SM-Chol20 bilayer, OH-Chol locates, on average, 0.8 Å lower in the interface than in the PC-Chol bilayer. Distributions of vertical locations of the oxygen atoms of phosphate and OH-Chol groups in SM-Chol20 and PC-Chol bilayers are shown in Fig. 7, *a* and *b*, for the upper and lower leaflets, respectively. The maxima of distributions for Op in both bilayers overlap, but the distribution for OH-Chol in the SM-Chol20 bilayer is shifted toward the bilayer core relative to that in the PC-Chol bilayer. Fig. 7 also shows that distributions for OH-Chol and Op in the PC-Chol bilayer are narrower than those in the SM-Chol20 bilayer. These indicate that the PC-Chol bilayer is a less dynamic system. In analogy to the previously observed correlation (32), one would expect the effect of the sterol ring on hydrocarbon chains to be stronger in the SM-Chol20 than in the PC-Chol bilayer. Indeed, at temperatures below the main phase-transition temperatures for pure SSM and 15SPC bilayers, the SM-Chol20 bilayer is in the liquid-ordered phase, whereas the PC-Chol bilayer is in the gel phase.

DISCUSSION

In this article, we present a comparative MD simulation study of the effect of Chol on sphingomyelin and phosphatidylcholine bilayers. Four bilayers with and without Chol were studied at two temperatures. Each contained the same number of phospholipid molecules, either SSM or 15SPC,

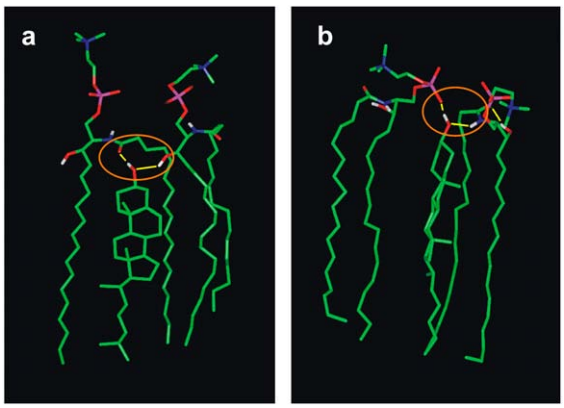

FIGURE 6 Examples of H-bonds (*ellipsed area*) between the OH-Chol group of one Chol molecule and two SSM molecules (*thin yellow lines*). (*a*) OH-Chol···SM-OH and OH-Chol···SM-OC H-bonds; (*b*) OH-Chol···SM-NH and OH-Chol···SM-Op H-bonds in the SM-Chol20 bilayer. The SSM and Chol molecules are in stick representation and standard colors.

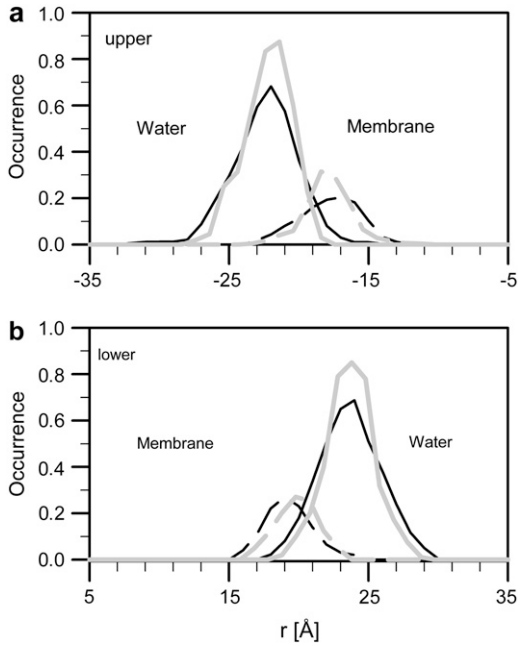

FIGURE 7 Distributions of vertical locations of the oxygen atoms of phosphate (*solid lines*) and OH-Chol (*dashed lines*) groups along the normal in SM-Chol20 (*black*) and PC-Chol (*gray*) bilayers for the upper (*a*) and lower (*b*) leaflets. Zero of the horizontal axis (not shown) indicates the middle of the hydrocarbon core of the bilayer.

and a varying number of Chol molecules. The bilayers comprised two groups. The first group consisted of two SSM-Chol bilayers, one containing 22 and the other 50 mol % Chol, and a 15SPC-Chol bilayer containing 22 mol % Chol. SSM and 15SPC have hydrocarbon chains of matching lengths and similar main phase-transition temperatures (~45°C). Simulations of these systems were carried out at 37°C. Their main purpose was to compare the effect of Chol on SSM and 15SPC bilayers at the same Chol concentration, at physiological temperature, and also to assess the effect of the increased Chol concentration (22 or 50 mol %) on the SSM bilayer. The second group consisted of a pure SSM and a SSM-Chol bilayer containing 22 mol % Chol. Simulations of these systems were carried out at 60°C to evaluate the effect of Chol on the SSM bilayer in the liquid-crystalline state.

Chol effects on the liquid-crystalline SSM bilayer

Entries in Table 1 concerning SM and SM-Chol20* bilayers as well as Figs. 4 and 5 indicate that Chol exerts both ordering and condensing effects on the SSM bilayer. In the SM-Chol20* bilayer, Chol induced the increase in the surface density of ~17%, in the average value of S_{mol} of ~40%, in the bilayer thickness (the P-P distance) of ~7% (3 Å), as well as the decrease in the chain tilt of ~30% (~6°) and in the number of *gauche* rotamers of ~30%. The Chol-induced increase of SSM hydrocarbon chains ordering as well as the bilayer thickness originate from the decrease of the average tilt of the chains and the probability of *gauche*.

PC-PC and PC-water interactions taking place at the membrane/water interface are correlated with the average surface area available to the PC headgroup (49). With increasing area, the number of inter-lipid interaction decreases (due to a larger inter-lipid distance) but the number of hydrating water molecules increases (due to a better access to PC polar groups). A similar correlation is observed in the SSM bilayers studied here. In the SM-Chol20* bilayer the average surface area available to the SSM headgroups is larger than in the SM bilayer and accordingly, the number of bound water molecules is larger and the number of direct SSM-SSM interactions via H-bonds and charge pairs is smaller. As a matter of fact, in the SM-Chol20* bilayer there is a competition between SSM and Chol to interact with SSM, so a meticulous comparison of the number of SSM-SSM interactions in both bilayers is not fully justified. The number of intermolecular H-bonds in the SM bilayer of 0.66/SSM falls into the range 0.41–0.8/SM obtained in other MD simulations of SSM or palmitoylSM (PSM) bilayers at ~50°C (11–13). The number of intramolecular H-bonds of 0.5/SSM is practically the same in SM and SM-Chol20* bilayers. This number is not far from those obtained in other MD simulations of SM and SM-Chol bilayers at ~50°C (11–13,34) ranging 0.59–1.1/SSM or PSM. Also Hyvönen and Kovanen (33) observed intramolecular H-bonds in the PSM bilayer at 37°C, but their number was not provided. However, the bonds observed in this study are made primarily between SM-OH and SM-OC, whereas in the studies cited above, primarily between SM-OH and O11 (cf. Fig. 1 *b*). Assuming that in all cases the sphingosine base of the SM molecule had *d-erythro-* (2S, 3R) configuration, as was pointed out in the Method section of this as well as Hyvönen and Kovanen (33) and Niemelä et al. (13) papers, a different SM-OH partner in intra-lipid H-bonding may result from conformational variations in the sphingosine base due to differences in the parameterization of the C4=C5 *trans* double bond and single bonds next to it. Validation of the parameterization used in this study is presented in our previous paper (52) where properties of a mono-*trans*-unsaturated bilayer are analyzed. Ramstedt and Slotte (53) studied the effect of the isomeric form of SM on the bilayer properties and showed that the surface area/SM in the bilayer is smaller for *d-erythro-* than for the racemic SM.

SSM-Chol bilayers at different temperatures

Khelashvili and Scott (34) compared properties of SSM-Chol bilayers containing ~30 mol % Chol and MD simulated at temperatures below (20°C) and above (50°C) T_m for a pure SSM bilayer of ~45°C. The bilayer thickness, hydrocarbon chains order as well as area/molecule were very similar in both systems indicating that the bilayers were in a similar state of fluidity. In this study, we compare SSM-Chol bilayers containing 22 mol % Chol and MD simulated at temperatures 37°C (SM-Chol20) and 60°C (SM-Chol20*). The bilayer thickness, hydrocarbon chains order, and SSM-SSM interactions in both bilayers are similar and only the surface density is slightly lower at lower temperature (Table 1). Thus, the results obtained by Khelashvili and Scott (34) for the SSM bilayers containing ~30 mol % Chol and our results obtained for SSM bilayers containing 22 mol % Chol are in full agreement, although they do not fully agree with x-ray diffraction results of Maulik and Shipley (48), who found that only at ~50 mol % Chol diffraction patterns of SSM-Chol bilayers are identical both below and above T_m for a pure SSM bilayer.

SSM-Chol bilayers at different Chol content

Entries in Table 1 concerning SM-Chol50 and SM-Chol20 bilayers indicate that when Chol content is increased from 22 to 50 mol %, the SSM chain order increases by ~18%. This increase is mainly due to an ~42% decrease of the chain tilt as the number of *gauche* rotamers is increased by ~9%. Most likely, this concomitant decrease of the chain tilt and increase of the number of *gauche* rotamers causes that the P-P distance of 46.5 Å is the same in both bilayers. The value 46.5 Å agrees perfectly with those obtained by x-ray diffraction at 58°C and 22°C for the SSM bilayer containing 50 mol % Chol, ranging from 46 to 47 Å (48). Our study

indicates additionally that the P-P distance in all SSM bilayers containing Chol is practically the same, irrespective of the Chol concentration and the bilayer temperature.

At the membrane/water interface of the SM-Chol50 bilayer, there are significantly fewer interlipid (Table 2) and more lipid-water interactions (Table 3) than at that of the SM-Chol20 bilayer. This is consistent with a larger SSM-SSM average distance in the SM-Chol50 bilayer (Table 1). The number of intramolecular interactions is slightly higher in the SM-Chol50 bilayer, probably to compensate for some of the missing intermolecular interactions.

Location of the OH-Chol in the bilayer interface

Our previous studies (20,32) as well as those of Karolis et al. (54), Smondyrev and Berkowitz (55,56), and Faure et al. (57) indicate that the effect of sterol on the bilayer is correlated with the average relative location of the sterol's hydroxyl group in the bilayer interface. The OH group of Echol in the DMPC-Echol bilayer and the OH-Chol group in the POPC-Chol bilayer are located 2–3 Å higher in the interfacial regions than is OH-Chol in the DMPC-Chol bilayer, and both Echol and Chol have smaller effects on DMPC and POPC bilayers, respectively, than does Chol on the DMPC bilayer (20,32). In the SSM bilayers containing Chol, OH-Chol is located 0.1–0.4 Å lower in the interface than in the DMPC-Chol bilayer, so the Chol effect on the SSM bilayer is expected to be somewhat larger. Indeed, when compared at the same Chol content (~20 mol %) and $T > T_m$, the condensing effect of Chol on the SSM bilayer is stronger (the surface density increases ~17% and ~10% in the SSM-Chol and DMPC-Chol (30) bilayers, respectively) but the ordering effect is comparable as the Chol-induced changes in S_{mol} and chain tilt are similar in both systems. The most pronounced difference between the Chol effect on SSM and DMPC bilayers is that Chol decreases the average number of *gauche* rotamers by ~30% in the SM-Chol20* bilayer, whereas in the DMPC-Chol bilayer the decrease is negligible (30).

The effect of the OH-Chol location on the bilayer properties is even more striking when the SSM-Chol bilayer is compared with the 15SPC-Chol bilayer at a temperature below the T_ms for pure SSM and 15SPC bilayers (Fig. 7). In the PC-Chol bilayer, the average vertical position of the OH-Chol in the interface is 0.8 Å higher. This difference in the position might, at first sight, seem small but it is very close to the vertical distance between two consecutive carbon atoms in the acyl chain. Due to this higher position, the effect of the sterol ring on the 15SPC chains is evidently too weak to modify the phase state of the PC-Chol bilayer, and at 37°C the PC-Chol bilayer remains in the gel phase. This is evidenced by the collective tilt of the PC chains and Chol, which is ~17° (cf. Equilibration), whereas the collective tilt of chains in the liquid-crystalline phase is zero. In contrast, the lower vertical position of Chol affects ''fluidity'' of the SSM chains, and at 37°C the SM-Chol20 bilayer is in the liquid-ordered phase. A deeper insertion of OH-Chol in the SM-Chol20 bilayer is stabilized by numerous H-bonds between OH-Chol and SSM polar groups that are located closer to the bilayer core, i.e., SM-OC, SM-OH and SM-NH groups. As 15SPC has no H-bond donor groups, it makes over three times fewer H-bonds with Chol, and additionally, the bonds are formed more often with the phosphate than with the carbonyl group (Table 4). Thus, OH-Chol is anchored higher in the interfacial region of the PC-Chol bilayer than in that of the SM-Chol bilayer. Once formed, H-bonds stabilize the position of OH-Chol in the bilayer and larger changes in both the location of the OH-Chol and the number of phospholipid-Chol H-bonds would not be expected if the simulation of the bilayer were continued.

The key result of this MD simulation study is demonstration that at 37°C, Chol at concentration 22 mol % is able to change the phase of the SSM bilayer from gel to liquid-ordered, whereas it is not able to change the phase of the 15SPC bilayer despite the fact that hydrocarbon chains of both SSM and 15SPC have the same lengths and the main phase-transition temperatures of SSM and 15SPC bilayers are 45°C (5) and 43°C (44), respectively. A plausible explanation, relating this observation to the location of OH-Chol in the bilayer interfacial region, is given above. By showing this, i.e., correlating the location of Chol with its ability to modify the membrane phase state, the study described here extends the results of previous studies that indicated a correlation between the location of a sterol molecule in the membrane and the strength of ordering and condensing effects of the sterol (20,32,54–57).

Saturated PCs with chains of unequal length (C(X):C(Y)PC) for which the normalized effective chain length difference, $\Delta C/CL$, is <0.42 (both the effective chain length difference $\Delta C = |X - Y + 1.5|$ and the effective length of the longer of the two acyl chains, CL, are expressed in C–C bond-length units) pack into a partially interdigitated bilayer at $T < T_m$ (58). This rule was found to be valid when the difference between numbers of carbon atoms in the two PC chains (ΔN) is an even number. If we assume, based on Marsh's study (59), that the same rule holds for odd ΔN, then one can expect that the pure 15SPC bilayer in the gel phase is partially interdigitated, as $\Delta C/CL$ for 15SPC is ~0.1. Partially interdigitated bilayers are highly ordered. However, by perturbing the acyl chain order, Chol can abolish both the phase transition and the interdigitated structure of the bilayer (60). Parameters characterizing the PC-Chol bilayer (Table 1 and Fig. 3) suggest that the bilayer is in the gel phase but does not form a partially interdigitated structure. Instead, the lipids in each bilayer leaflet are collectively tilted to compensate for the mismatch of their acyl chains. When the temperature of the PC-Chol bilayer was elevated to 90°C, the collective tilt of the acyl chains disappeared within 10 ps of MD simulation (Supplementary Material, Fig. S8). One of the biological consequences of the observation that at the same temperature and Chol content the 15SPC-Chol bilayer

is in the gel phase, whereas the SSM-Chol bilayer is in the liquid-ordered phase, might be at most a very rare occurrence of 15SPC in the biomembrane. Indeed, saturated PCs with an odd ΔN and, particularly, with 15 carbon atoms in the γ-chain are quite uncommon.

SUPPLEMENTARY MATERIAL

An online supplement to this article can be found by visiting BJ Online at http://www.biophysj.org.

This study was supported in part by grant 6P04A03121 from the Polish Committee for Scientific Research, Warsaw, Poland. All calculations were performed in the Academic Computational Centre Cyfronet, Kraków, Poland, computational grant number KBN/SGI_ORGIN200/UJ/004/2000. T.R. holds Marie Curie Intra-European Fellowship 024612-Glychol.

REFERENCES

1. Simons, K., and E. Ikonen. 1997. Functional rafts in cell membranes. *Nature*. 387:569–572.
2. Pandit, S. A., S. Vasudevan, S. W. Chiu, R. J. Mashl, E. Jacobsson, and H. L. Scott. 2004. Sphingomyelin-cholesterol domains in phospholipid membranes: atomistic simulation. *Biophys. J.* 87:1092–1100.
3. Pandit, S. A., E. Jacobsson, and H. L. Scott. 2004. Simulation of the early stages of nano-domain formation in mixed bilayers of sphingomyelin, cholesterol, and dioleoylphosphatidylcholine. *Biophys. J.* 87:3312–3322.
4. Ramstedt, B., and P. Slotte. 2002. Membrane properties of sphingomyelins. *FEBS Lett.* 531:33–37.
5. Koynova, R., and M. Caffrey. 1995. Phases and phase transitions of the sphingolipids. *Biochim. Biophys. Acta.* 1255:213–236.
6. Robinson, A. J., W. G. Richards, P. J. Thomas, and M. M. Hann. 1995. Behavior of cholesterol and its effect on head group and chain conformations in lipid bilayers: a molecular dynamics study. *Biophys. J.* 68:164–170.
7. Tu, K., M. L. Klein, and D. J. Tobias. 1998. Constant-pressure molecular dynamics investigation of cholesterol effects in a dipalmitoylphosphatidylcholine bilayer. *Biophys. J.* 75:2147–2156.
8. Pasenkiewicz-Gierula, M., T. Róg, K. Kitamura, and A. Kusumi. 2000. Cholesterol effects on the phosphatidylcholine bilayer polar region: a molecular simulation study. *Biophys. J.* 78:1376–1389.
9. Veiga, M. P., J. L. R. Arrondo, F. M. Goni, A. Alonso, and D. Marsh. 2001. Interaction of cholesterol with sphingomyelin in mixed membranes containing phosphatidylcholine, studied by spin-label ESR and IR spectroscopies. A possible stabilization of gel-phase sphingolipid domains by cholesterol. *Biochemistry.* 40:2614–2622.
10. Kan, C. C., Z. S. Ruan, and R. Bittman. 1991. Interaction of cholesterol with sphingomyelin in bilayer membranes: evidence that hydroxyl group of sphingomyelin does not modulate the rate of cholesterol exchange between vesicles. *Biochemistry.* 30:7759–7766.
11. Mombelli, E., R. Morris, W. Taylor, and F. Fraternali. 2003. Hydrogen-bonding propensities of sphingomyelin in solution and in a bilayer assembly: a molecular dynamics study. *Biophys. J.* 84:1507–1517.
12. Chiu, S. W., S. Vasudevan, E. Jakobsson, R. J. Mashl, and H. L. Scott. 2003. Structure of sphingomyelin bilayers: a simulation study. *Biophys. J.* 85:3624–3635.
13. Niemelä, P., M. T. Hyvönen, and I. Vattulainen. 2004. Structure and dynamics of sphingomyelin bilayer: insight gained through systematic comparison to phosphatidylcholine. *Biophys. J.* 87:2976–2989.
14. Talbott, C. M., I. Vorobyov, D. Borchman, K. G. Taylor, D. B. DuPré, and M. C. Yappert. 2000. Conformational studies of sphingolipids by NMR spectroscopy. II. Sphingomyelin. *Biochim. Biophys. Acta.* 1467: 326–337.
15. Holopainen, J. M., A. J. Metso, J. Mattila, A. Jutila, and P. K. J. Kinnunen. 2004. Evidence for the lack of a specific interaction between cholesterol and sphingomyelin. *Biophys. J.* 86:1510–1520.
16. Urbina, J. A., B. Moreno, W. Arnold, C. H. Taron, P. Orlean, and E. Oldfield. 1998. A carbon-13 nuclear magnetic resonance spectroscopic study of inter-proton pair order parameters: a new approach to study order and dynamics in phospholipid membrane systems. *Biophys. J.* 75:1372–1383.
17. Chiu, S. W., E. Jakobsson, and H. L. Scott. 2001. Combined Monte Carlo and molecular dynamics simulation of hydrated dipalmitoyl-phosphatidylcholine-cholesterol lipid bilayers. *J. Chem. Phys.* 114:5435–5443.
18. Chiu, S. W., E. Jakobsson, and H. L. Scott. 2001. Combined Monte Carlo and molecular dynamics simulation of hydrated lipid-cholesterol lipid bilayers at low cholesterol concentration. *Biophys. J.* 80:1104–1114.
19. Smaby, J. M., M. Momsen, H. L. Brockman, and R. E. Brown. 1997. Phosphatidylcholine acyl unsaturation modulates the decrease in interfacial elasticity induced by cholesterol. *Biophys. J.* 73:1492–1505.
20. Róg, T., and M. Pasenkiewicz-Gierula. 2006. Cholesterol effects on a mixed-chain phosphatidylcholine bilayer: a molecular dynamics simulation study. *Biochimie.* 88:449–460.
21. Ramstedt, B., and J. P. Slotte. 1999. Interaction of cholesterol with sphingomyelins and acyl-chain-matched phosphatidylcholines: a comparative study of the effect of the chain length. *Biophys. J.* 76:908–915.
22. Sankaram, M. B., and T. E. Thompson. 1990. Interaction of cholesterol with various glycerophospholipids and sphingomyelin. *Biochemistry.* 29:10670–10675.
23. Smaby, J. M., H. L. Brockman, and R. E. Brown. 1994. Cholesterol's interfacial interactions with sphingomyelins and phosphatidylcholines: hydrocarbon chain structure determines the magnitude of condensation. *Biochemistry.* 33:9135–9142.
24. Chiu, S. W., E. Jakobsson, R. J. Mashl, and H. L. Scott. 2002. Cholesterol-induced modifications in lipid bilayers: a simulation study. *Biophys. J.* 83:1842–1853.
25. Smondyrev, A. M., and M. L. Berkowitz. 1999. Structure of dipalmitoylphosphatidyl-choline/cholesterol bilayer at low and high cholesterol concentrations: a molecular dynamics simulation. *Biophys. J.* 77:2075–2089.
26. Smondyrev, A. M., and M. L. Berkowitz. 2001. Effects of oxygenated sterol on phospholipid bilayer properties: a molecular dynamics simulation. *Chem. Phys. Lipids.* 112:31–39.
27. Hofsäß, C., E. Lindahl, and O. Edholm. 2003. Molecular dynamics simulation of phospholipid bilayer with cholesterol. *Biophys. J.* 84: 2192–2206.
28. Falck, E., M. Patra, M. Karttunen, M. T. Hyvönen, and I. Vattulainen. 2004. Lessons of slicing membranes: interplay of packing, free area, and lateral diffusion in phospholipid/cholesterol bilayers. *Biophys. J.* 87:1076–1091.
29. Falck, E., M. Patra, M. Karttunen, M. T. Hyvönen, and I. Vattulainen. 2004. Impact of cholesterol on voids in phospholipid membranes. *J. Chem. Phys.* 121:12676–12680.
30. Róg, T., and M. Pasenkiewicz-Gierula. 2001. Cholesterol effects on the phosphatidylcholine bilayer nonpolar region: a molecular simulation study. *Biophys. J.* 81:2190–2202.
31. Róg, T., and M. Pasenkiewicz-Gierula. 2001. Cholesterol effects on the membrane packing and condensation: a molecular simulation study. *FEBS Lett.* 502:68–71.
32. Róg, T., and M. Pasenkiewicz-Gierula. 2003. Effects of epicholesterol on the phosphatidylcholine bilayer: a molecular simulation study. *Biophys. J.* 84:1818–1826.
33. Hyvönen, M. T., and P. T. Kovanen. 2003. Molecular dynamics simulation of sphingomyelin bilayer. *J. Phys. Chem. B.* 107:9102–9108.
34. Khelashvili, G. A., and H. L. Scott. 2004. Combined Monte Carlo and molecular dynamics simulation of hydrated 18:0 sphingomyelin-cholesterol lipid bilayers. *J. Chem. Phys.* 120:9841–9847.
35. Nyholm, P., I. Pascher, and S. Sundell. 1990. The effect of hydrogen bonds on the conformation of glycosphingolipids. methylated and

unmethylated cerebroside studied by X-ray single crystal analysis and model calculations. *Chem. Phys. Lipids.* 52:1–10.

36. Case, D. A., D. A. Pearlman, J. W. Caldwell, T. E. Cheatham III, W. S. Ross, C. Simmerling, T. A. Darden, K. M. Merz, R. V. Stanton, A. L. Cheng, J. J. Vincent, M. Crowley, et al. 1997. AMBER 5.0. University of California, San Francisco, CA.
37. Jorgensen, W. L., and J. Tirado-Rives. 1988. The OPLS potential functions for proteins. Energy minimizations for crystals of cyclic peptides and crambin. *J. Am. Chem. Soc.* 110:1657–1666.
38. Pasenkiewicz-Gierula, M., Y. Takaoka, H. Miyagawa, K. Kitamura, and A. Kusumi. 1999. Charge pairing of headgroups in phosphatidylcholine membranes: a molecular dynamics simulation study. *Biophys. J.* 76:1228–1240.
39. Jorgensen, W. L., J. Chandrasekhar, J. D. Madura, R. W. Impey, and M. L. Klein. 1983. Comparison of simple potential functions for simulating liquid water. *J. Chem. Phys.* 79:926–935.
40. Ryckaert, J. P., G. Ciccotti, and H. J. C. Berendsen. 1977. Numerical integration of the Cartesian equations of motion of a system with constraints: molecular dynamics of *n*-alkanes. *J. Comp. Phys.* 23:327–341.
41. Egberts, E., S.-J. Marrink, and H. J. C. Berendsen. 1994. Molecular dynamics simulation of a phospholipid membrane. *Eur. Biophys. J.* 22: 423–436.
42. Essmann, U., L. Perera, M. L. Berkowitz, T. Darden, H. Lee, and L. G. Pedersen. 1995. A smooth particle mesh Ewald method. *J. Chem. Phys.* 103:8577–8593.
43. Maulik, P., P. Spirada, and G. Shipley. 1991. Structure and thermotropic properties of hydrated N-stearoyl sphingomyelin bilayer membranes. *Biochim. Biophys. Acta.* 1062:211–219.
44. Huang, C. H., and S. S. Li. 1999. Calorimetric and molecular mechanics studies of the thermotropic phase behavior of membrane phospholipids. *Biochim. Biophys. Acta.* 1422:273–307.
45. Berendsen, H. J. C., J. P. M. Postma, W. F. van Gunsteren, A. DiNola, and J. R. Haak. 1984. Molecular dynamics with coupling to an external bath. *J. Chem. Phys.* 81:3684–3690.
46. Tristram-Nagle, S., R. Zhang, R. M. Suter, C. R. Worthington, W.-J. Sun, and J. Nagle. 1993. Measurement of chain tilt angle in fully hydrated bilayers of gel phase lecithins. *Biophys. J.* 64:1097–1109.
47. Tu, K., D. J. Tobias, J. K. Blasie, and M. L. Klein. 1996. Molecular dynamics investigation of the structure of a fully hydrated gel-phase dipalmitoylphosphatidylcholine bilayer. *Biophys. J.* 70:595–608.
48. Maulik, P., and G. Shipley. 1996. Structure and thermotropic properties of hydrated N-stearoyl sphingomyelin bilayer membranes. *Biophys. J.* 70:2256–2265.
49. Murzyn, K., T. Róg, G. Jezierski, Y. Takaoka, and M. Pasenkiewicz-Gierula. 2001. Effects of phospholipid unsaturation on the membrane/water interface: a molecular simulation study. *Biophys. J.* 81:170–183.
50. Vainio, S., M. Jansen, M. Koivusalo, T. Róg, M. Karttunen, I. Vattulainen, and E. Ikonen. 2006. Significance of sterol structural specificity. *J. Biol. Chem.* 281:348–355.
51. Pasenkiewicz-Gierula, M., Y. Takaoka, H. Miyagawa, K. Kitamura, and A. Kusumi. 1997. Hydrogen bonding of water to phosphatidylcholine in the membrane as studied by a molecular dynamics simulation: location, geometry and lipid-lipid bridging via hydrogen bonded water. *J. Chem. Phys.* 101:3677–3691.
52. Róg, T., K. Murzyn, R. Gurbiel, K. Kitamura, A. Kusumi, and M. Pasenkiewicz-Gierula. 2004. Effects of phospholipid unsaturation on the structure and dynamics of the hydrocarbon core of the membrane. A molecular simulation study. *J. Lip. Res.* 45:326–336.
53. Ramstedt, B., and J. P. Slotte. 1999. Comparison of the biophysical properties of racemic and *d-erythro*-N-acyl sphingomyelins. *Biophys. J.* 77:1498–1506.
54. Karolis, C., H. G. Coster, T. C. Chilcott, and K. D. Barrow. 1998. Differential effects of cholesterol and oxidised-cholesterol in egg lecithin bilayers. *Biochim. Biophys. Acta.* 1368:247–255.
55. Smondyrev, A. M., and M. L. Berkowitz. 2001. Molecular dynamics simulation of the structure of dimyristoylphosphatidylcholine bilayers with cholesterol, ergosterol, and lanosterol. *Biophys. J.* 80:1649–1658.
56. Smondyrev, A. M., and M. L. Berkowitz. 2000. Molecular dynamics simulation of dipalmitoylphosphatidylcholine membrane with cholesterol sulfate. *Biophys. J.* 78:1672–1680.
57. Faure, C., J. F. Tranchant, and E. J. Dufourc. 1996. Comparative effects of cholesterol and cholesterol sulfate on hydration and ordering of dimyristoylphosphatidylcholine membranes. *Biophys. J.* 70:1380–1390.
58. Huang, C., and J. T. Mason. 1986. Structure and properties of mixed-chain phospholipid assemblies. *Biochim. Biophys. Acta.* 864:423–470.
59. Marsh, D. 1993. Analysis of the bilayer phase transition temperatures of phosphatidylcholines with mixed chains. *Biophys. J.* 61:1036–1040.
60. Chong, P. L.-G., and D. Choate. 1989. Calorimetric studies of the effect of cholesterol on the phase transition of C(18):C(10) phosphatidylcholine. *Biophys. J.* 55:551–556.